Coalescence during bubble formation from two neighbouring pores in a non-Newtonian liquid

Georgios A. Oikonomou, Agathoklis D. Passos, Aikaterini A. Mouza and Spiros V. Paras*

Laboratory of Chemical Process and Plant Design
Department of Chemical Engineering
Aristotle University of Thessaloniki
Thessaloniki, Greece
**Corresponding author: Tel.: +30 2310 996174; Email: paras@auth.gr*

Abstract

This work expands our previous study that experimentally investigates the coalescence of bubbles formed from two adjacent μ-tubes into a static non-Newtonian liquid, which follows the Herschel-Bulkley model. A fast video recording technique was employed for the visual observations of the phenomena and bubble size measurements. The aim of the present work is to interpret the phenomena by numerically investigating the flow field around a typical bubble formed from a μ-tube. The numerical model has been successfully validated by performing a series of relevant experiments, using deionized water as Newtonian liquid and aqueous glycerin solutions with a small amount of xanthan gum as typical shear-thinning non-Newtonian liquids. The *CFD* results reveal that the shear rate around an under-formation bubble attains relatively low values (<180s^{-1}) resulting to dynamic viscosity values 100% higher than the asymptotic value of the respective liquid. This finding confirms the notion that the low coalescence frequency found in our experiments may be attributed to high viscosity values a fact that is also encountered in bubble formation into highly viscous Newtonian liquids.

Keywords: *coalescence, μ-tube, non-Newtonian liquid, CFD*

1. Introduction

This work stems from the need to interpret the phenomena affecting bubble formation in bubble columns equipped with porous sparger and loaded with a non-Newtonian shear thinning liquid. As it is known, bubble columns are widely used as gas-liquid contactors in chemical and biochemical applications, since they have a large gas-liquid interface and consequently they offer superior heat and mass transfer characteristics. Apart from their high energy efficiency and good mass and heat transfer characteristics, due to their compactness and the lack of moving parts, they require little maintenance and have low operating cost [1].

The porous plates hold advantages over the other types of spargers used as gas distributors, since they produce numerous and smaller bubbles, offering a greater gas–liquid contact area [1]. An important parameter affecting bubble column efficiency is the extent of the interfacial area available for mass and heat transfer [2], which in turn is a function of gas hold up, i.e. the volumetric gas fraction, and the bubble size distribution. It is also known that bubble size distribution is strongly affected by breakage and coalescence phenomena occurring on to or in the vicinity of the sparger area [1]. It is also regarded that two neighboring pores can be adequately simulated by two adjacent microtubes (μ-tubes) located at various distances apart from each other (Fig.1). Consequently, it is important to comprehend bubble formation and coalescence phenomena at the microscopic level in order to be able to interpret the phenomena occurring during bubble formation on the sparger area [1].

Bubble formation starts when the gas phase pressure under a pore attains a higher value than the hydrostatic and the capillary pressure of the pore [3]. The capillary pressure is given by:

$$\Delta P = \frac{2\sigma}{r_p} \quad (1)$$

where σ is the surface tension and r_p is the pore radius. Bubble formation is a two stage process, namely the ***expansion*** stage, during which the bubble remains attached to the porous, and the ***detachment*** stage. Obviously, the rate of growth of an under-formation bubble depends on the gas flow rate. During the expansion stage, two under formation bubbles might collide and coalesce via a three-step process, i.e. collision of the bubbles, drainage of the liquid film trapped between the bubbles and finally rupture of the liquid film via an instability mechanism [1]. If the gas flow rate is low, the contact time is less than the drainage time and no breakage occurs. On the other hand, if gas flow rate is high, bubbles may detach before the drainage occurs [1].

Shear thinning non-Newtonian fluids are widely used in industry and are involved in several bubble column applications, e.g. polymer solutions and melts, liquid crystals, gels, suspensions, emulsions, micellar solutions, slurries, foams, etc. In this case the liquid viscosity is not constant but depends on the shear rate, i.e. it decreases when the shear rate increases.

This work extents our previous work [1] that refers to Newtonian liquids and examines coalescence during bubble formation at two neighboring pores. Recently, in our Lab we studied [3] formation and coalescence of bubbles generated from two adjacent μ-tubes into shear thinning non-Newtonian liquids, namely various aqueous glycerin solutions containing a small amount of xanthan gum. The results obtained by processing fast video recordings (i.e. 3000fps), reveal that for a wide range of gas flow rates there is practically no coalescence. Anastasiou et al. [4] who performed experiments in bubble columns loaded with non-Newtonian shear thinning liquids, reports that the behavior of the non-Newtonian liquids is similar to that of a high viscosity liquid; e.g. they observed bubble clusters. As the viscosity of a non-Newtonian shear thinning liquid covers a wide range of values that depends on the shear rate, it is reason-

able to assume that the shear rate around an under formation bubble is relatively ***low***, leading to high viscosity values that in turn inhibit coalescence. To verify this assumption, we must investigate the shear rate distribution around an under formation bubble during the expansion and detachment stages. In the last few years several attempts have been made to numerically investigate bubble flow characteristics in non-Newtonian fluids [e.g. 5, 6, 7].

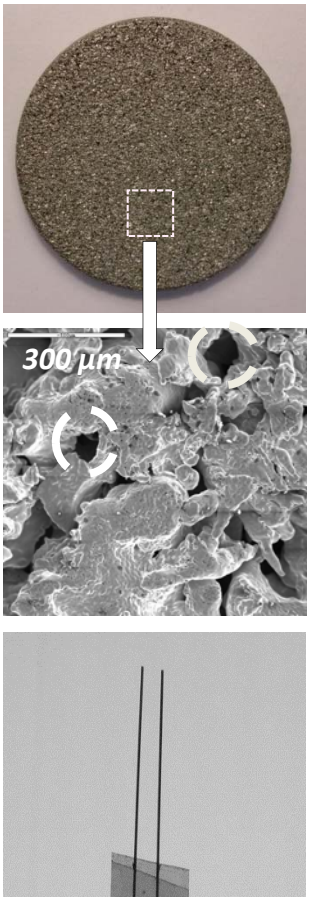

Figure 1: Simulation of two adjacent pores of a sparger by two μ-tubes. (a) sparger, (b) typical pores, (c) μ-tubes.

Thus the ***aim*** of this study to numerical simulate the flow around a typical bubble formatted from a μ-tube in a non-Newtonian shear thinning liquid which follows the *Herschel-Bulkley* viscosity model (Eqn. 2):

$$\tau = \tau_0 + k \cdot \dot{\gamma}^n \quad (2)$$

where τ_0 is the yield stress, k the consistency factor and n the flow index [8].

2. Numerical procedure

Nowadays Computational Fluid Dynamics (*CFD*) with the improvement of numerical algorithms and the enhancement of the computing power can provide a better physical understanding of two-phase flow problems like single bubble rising behavior, replacing expensive and laborious experiments. In the present study the bubble formation is numerically investigated using the *ANSYS Fluent*® 15.0 package and the *Volume of Fluid (VOF)* method.

2.1. CFD model

The rise of a bubble in a liquid is affected by numerus parameters such as the properties of the gas-liquid system (density, viscosity, surface tension) and the operating conditions (temperature, pressure, gravity). As the bubble flow can be considered axisymmetric, a 2D computational domain with a perpendicular symmetry axis is used as simplification (Fig. 2). In this way, the constructed grid requires fewer cells, so the simulation needs less computing power and time. The dimensions of the domain (Fig. 2) are 1.5cm height by 5mm width. In order to avoid wall effects, the computational domain is wide enough, since total width is more than half of its height [e.g. 7, 9].

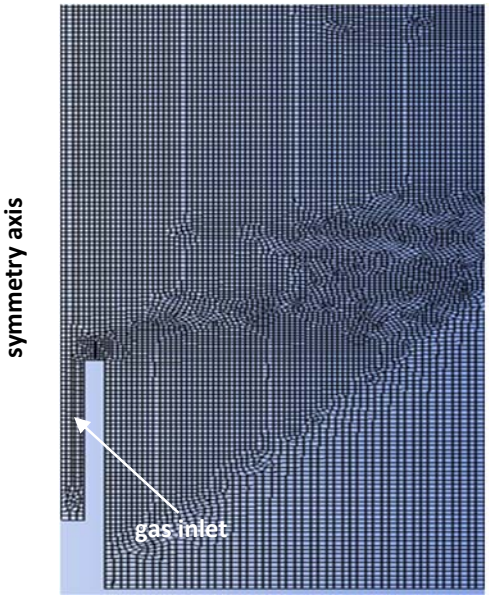

Figure 2: Computational domain.

The stainless steel μ-tube has an inner diameter of 110μm and outer diameter of 50μm which correspond to the dimensions of the experimental capillaries employed in our previous experimental work [3]. To properly capture the shape of the bubble it was necessary to have a relatively fine grid close to the gas inlet, where important phenomena (expansion, detachment and flow of the bubble) are expected (Fig. 2). For this purpose cell width is set to 1.3μm. In the rest of the computational domain, each cell has a width of 1.9μm, using a growth rate algorithm. The final grid consists of 174,000 cells (quadrilateral mesh type) and it is result of grid dependence study, in order to find the optimized number of cells.

To track the motion of a single bubble generated from the μ-tube in a stagnant liquid, the *VOF* model used is considered appropriate for modelling two-phase flows. More precisely the *VOF* model is suitable for immiscible fluids where the position of the interface is important [7]. This model consists of the continuity momentum equations for the two phases, which for an incompressible fluid can be written as:

$$\nabla \vec{V} = 0 \quad (3)$$

$$\rho(F)\left(\frac{\partial \vec{V}}{\partial t} + \nabla \vec{V}.\vec{V}\right) = -\nabla P + \rho(F)\vec{g} + \nabla\left[2\mu(F)\vec{D}\right] + \vec{F_s} \quad (4)$$

where ρ is the fluid density, $\vec{V}$ the velocity vector of the fluid, P the pressure, $\vec{F_s}$ the body force and μ the dynamic viscosity. The strain rate tensor, $\vec{D}$ is given by:

$$\vec{D} = \frac{1}{2}(\nabla\vec{V} + \nabla\overrightarrow{V^T}) \quad (5)$$

The volume fraction (F) is defined as the fraction of the liquid inside a cell and takes the value of 0 for a pure gas cell, 1 if the cell is filled with liquid and between 0 and 1 if there is a gas-liquid interface in the cell. The volume fraction equation is not solved for the primary phase, since F is constant and takes the value of 1 [7]. The tracking of the interface between the phases is accomplished by the solution of a continuity equation for the volume fraction of one (or more) of the phases. The volume fraction equation is defined as follows:

$$\frac{\partial F}{\partial t} + \nabla\left(\vec{V}F\right) = 0 \quad (6)$$

Since bubble rise is a surface tension dominated flow, to obtain a highly accurate curvature calculation, explicit scheme and Coupled Level Set are selected in the *VOF* model inputs.

In this study, the governing equations are solved using a pressure based solver. So, the pressure–velocity coupling equation is solved using the *SIMPLEC* algorithm. To obtain the face fluxes whenever a cell is completely filled with one phase or another and so track the interface, the *Geometric Reconstruction* scheme is used. This scheme is appropriate for time-dependent problems. The pressure interpolation scheme used is *PRESTO!,* which is suitable for multiphase models. Seeking for higher accuracy of the quantities at the cell faces, second order upwind is selected as the momentum discretization scheme. The time step and the maximum number of iterations per time step used for the simulation is 4.4μs and 25 respectively. For the needs of the present study a computer cluster that consists of 56 *AMD* cores and 196GB of *RAM* is used, while the time for one run varied from 36 to 48h.

The detachment time and the shear rate distribution around an under-formation air bubble are calculated for various liquids. Deionized water (Newtonian) and aqueous glycerin solutions with a small amount of xanthan gum (0.035g/100ml) (non-Newtonian fluids) are selected as the liquid phase. The properties of all liquids employed in this study are summarized in Table 1. For all the non-Newtonian liquids in the experiments, viscosity was measured with a magnetic rheometer (*AR-G2, TA Instruments*®). Surface tension was measured using a pendant drop technique (*KSV® CAM 200*).The non-Newtonian liquids used follow the *Herschel-Bulkley* model (Eqn. 2). The viscosity *vs*. shear rate curve for *G2* is presented in Fig. 3. The constant viscosities of the Newtonian liquids $G2_N$ and $G3_N$ are also shown for comparison.

Table 1: Solutions used as liquid phase.

Liquids	Symbol	Viscosity *mPa·s*	Surface tension *mN/m*
Water*	*W*	1.0	72.8
Aqueous Glycerin soln + xanthan gum	*G1*	2.3 - 55.0	70.0
Aqueous Glycerin soln + xanthan gum	*G2*	7.0 - 63.0	67.0
Aqueous Glycerin soln*	$G2_N$	13.0	67.0
Aqueous Glycerin soln*	$G3_N$	50.0	66.0

**Newtonian*

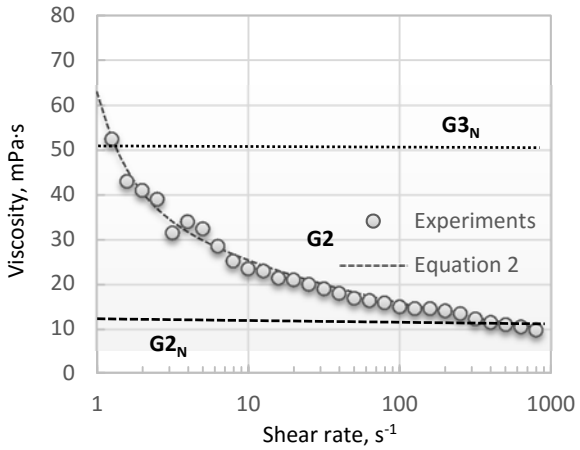

Figure 3: Viscosity as a function of shear rate (*G2*) and viscosity of the Newtonian $G2_N$ and $G3_N$.

2.2. CFD code validation

The code accuracy and reliability of the numerical model are validated by performing a series of three experiments and the corresponding simulations, in order to estimate the divergence in bubble equivalent diameter and in detachment time from the μ-tube. The experimental setup (Fig. 4) is the same as the one used for bubble coalescence study [3], but in this case only one μ-tube is used. All three experiments were conducted at temperature of (20 ±1^{O}C) and ambient pressure. Air was selected as gas phase to be inserted from the μ-tube.

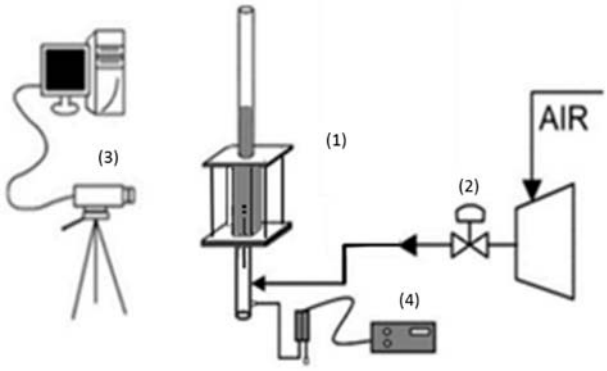

Figure 4: Experimental setup for bubble formation study. 1: Test section, 2: Valve, 3: High-speed video camera, 4: Pressure transducer.

The phenomena are captured by a high-speed digital video camera (*Fastec HighSpec4*). Recording rate was set to 3000fps, while the test section containing the μ-tube was standing between the camera and the lighting system. Detachment time and equivalent diameter of the bubbles are measured using a suitable software (*Redlake MotionScope*®). Moreover, since the minute flow rate of the air is extremely difficult to be measured with a conventional flow meter, it is estimated by calculating the bubble growth rate from the acquired images during a bubble formation. This flow rate was used as input to the numerical simulations. The pressure level of the gas chamber, which is located underneath the test section, during bubble formation is also constant and it is monitored by a differential pressure transducer.

The detachment time is the time elapsed between incipient bubble formation and the moment the bubble is detached from the μ-tube. The bubble equivalent diameter is given by Eqn. 7:

$$d_b = \sqrt[3]{L^2 H} \quad (7)$$

where H & L are the major and minor axes of the ellipsoid observed at the time of detachment (Fig. 5). 100 bubbles were measured to estimate the equivalent diameter, d_b.

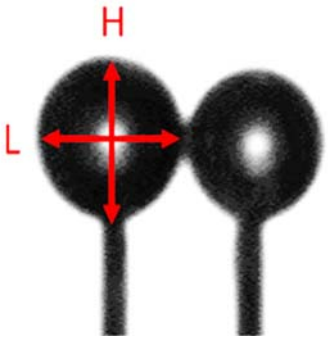

Figure 5: Geometrical characteristics of a bubble.

The experimental and numerical results are found to be in excellent agreement for the same air flow rate values (Q_G), i.e. better than 5%, (Table 2), both in terms of detachment time and equivalent diameter, for all liquids used. This small discrepancy may be attributed to the uncertainty of the bubble measuring procedure. Yet, this agreement verifies that the flow rate measuring method used is reliable.

Typical comparison between the experimental and the numerical results are presented for the expansion stage (Fig. 6) and the detachment stage (Fig. 7) for the non-Newtonian fluid *G2*. In conclusion the *CFD* code can predict the flow characteristics during bubble formation with reasonable accuracy.

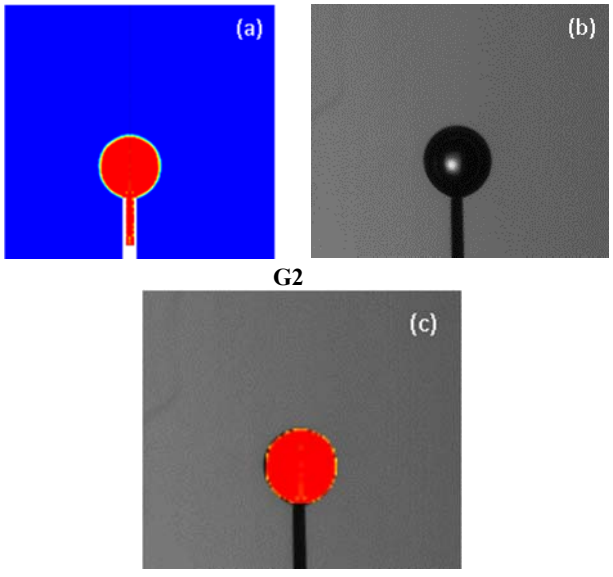

Figure 6: Typical bubble shape during expansion: (a) *CFD* simulation (b) experiment and (c) comparison (*G2*), Q_G=0.01cm^3/s.

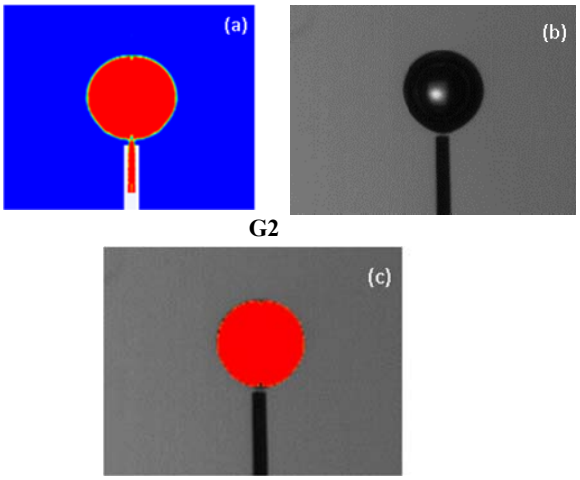

Figure 7: Typical shape of bubble at detachment: (a) *CFD* simulation (b) experiment and (c) comparison (*G2*), Q_G=0.01cm^3/s.

Table 2: Code validation results.

		Detachment time, *s*		d_b ,*mm*	
Liquid	Q_G *cm^3/s*	Expr	CFD	Expr	CFD
Water	0.002	0.215	0.211	1.95	1.90
G1	0.006	0.149	0.155	1.15	1.18
G2	0.010	0.136	0.140	1.34	1.40

3. Results

As it is already mentioned, bubble coalescence mechanism is a three-step process [1]:

- the two bubbles approach to within a distance of 1–10μm,
- the liquid layer between the bubbles is further thinning to a value of about 0.01μm and
- the thin liquid layer ruptures via an instability mechanism.

The initial experiments [3] reveal that the interactions between under-formation bubbles as well as the coalescence time depend strongly on the liquid properties, the distance between the tubes and the gas flow rate. It is also known [1] that the coalescence time, is inversely proportional to the viscosity of the liquid phase. Moreover, Kazakis et al. [1] report that the coalescence probability depends on the hydrodynamics of drainage of the liquid film between the two bubbles, the surface properties and the external flow. Thus, the **liquid viscosity** and the bubble residence time on the μ-tube are two opposing factors affecting bubble coalescence.

It is known that the primary force that keeps the bubble attached on the μ-tube is the surface tension, but as the gas flow rate increases, gas momentum force prevails. Consequently, the contact time of the two bubbles is less than the coalescence time, or more precicely the time the bubbles remain attached to the μ-tube is not adequate for the the liquid film to drain [10]. Also, when the gas flow rate increases, the growth rate of an under-formation bubble increases and as a result the shear rate values generated around the bubble also increase. Therefore,

when the forming bubble is surrounded by a non-Newtonian liquid, the liquid phase viscosity around the bubble is suspectible to the shear rate values.

In a previous work [3] we studied the evolution of bubbles formed in various ***non-Newtonian*** liquids from two μ-tubes placed at different distances apart from each other, namely 200μm and 700μm. For the longest distance, as expected, the coalescence frequency is very low, i.e. less than 10%, regardless of the gas flow rate or the type of liquid used. In this case the bubbles collide at a late stage of their expansion process and therefore there is not adequate time for the liquid film drainage. The bubbles expand, come in contact and finally detach without coalesence. On the other hand, when the distance between the tubes is 200μm, the bubbles collide at an early expansion stage.

Figure 8 depicts a typical sequence of bubble formation from two μ-tubes placed 200μm apart from each other, for various liquids. The experiments performed with Newtonian fluids ($G2_N$, $G3_N$) reveal that when the liquid viscosity is low the coalesence frequency approaches 100% (Fig. 8a), but for high viscosity values (e.g. μ=50μPa·s) practically no coalesence is observed (Fig. 8b). The non-Newtonian behavior (Fig. 8c) is similar to that of the high viscosity liquid $G3_N$.

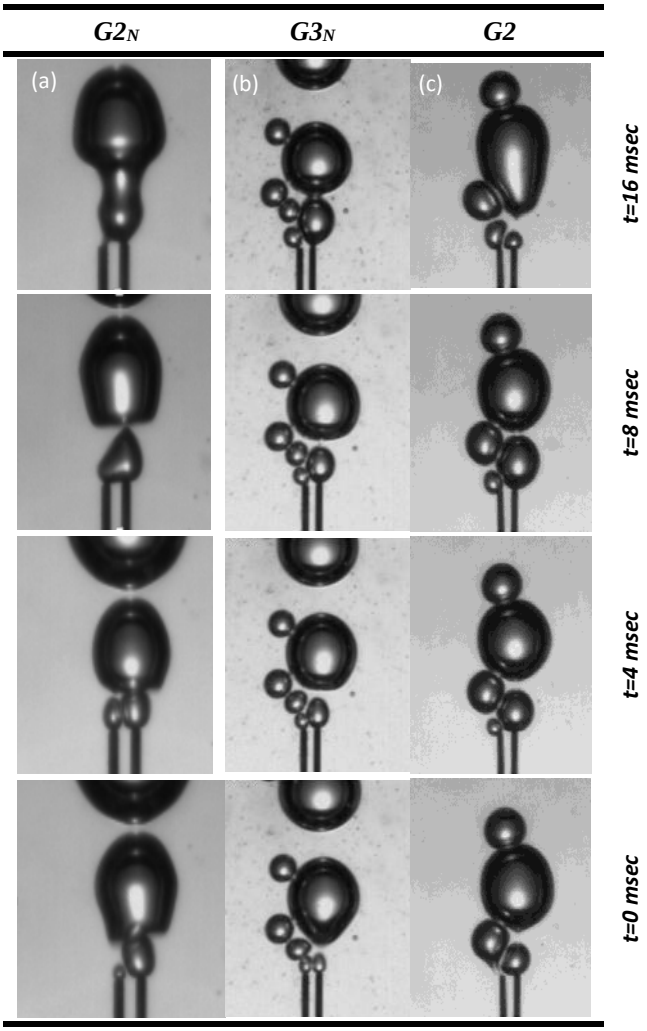

Figure 8: Bubble formation sequence from two adjacent μ-tubes 200μm apart, for (a) $G2_N$, (b) $G3_N$ *and* (c) *G2*, Q_G=0.10cm^3/s [3].

It is therefore reasonable to assume that the shear rate values exerted to the non-Newtonian liquid during the expansion stage are relatively low resulting to higher viscosity values according to Fig 3. To verify this assumption we performed relevant *CFD* simulations.

Using the validated *CFD* code, the shear rate distribution around an under-formation bubble is calculated for various air flow rates. The corresponding viscosity distribution can be estimated, using the viscosity curve each shear thinning liquid employed. The simulations reveal that for all liquids used, the shear rate around the bubble remains practically constant during the expansion and detachment stages. This observation is expected since the shear rate depends mainly on the rate of bubble growth which in turn depends on the constant gas flow rate during each "experiment". Figure 9 shows the distribution of the shear rate values around a bubble during the expansion and the detachment stages for the *G2* solution at Q_G=0.10cm^3/s. Similar results are also obtained for solution *G1*. Obviously, the shear rate exerted due to the bubble growth affects only the area in the vicinity of the bubble attaining relatively low values (<180 s^{-1}). This low shear rate, or equally high viscosity area, affects the mechanism of bubble colision.

While the bubble is being formated, shear-rate attains higher values in the horizontal direction, i.e. around 150-180s^{-1}, as shown in Fig. 9 and according to Fig. 8, bubbles interact through this direction. Consequently, shear rate at the area of buble side edges is important to be estimated.. Bubble coalescence is mostly affected by the values of shear rate in this particular area. So, as shear rate do not reach infinite values, viscosity takes higher values according to Fig. 3, both for expansion and detachment stages.

By comparing the shear rate distribution between expansion and detachment stage, it can be noticed that greater amount of the shear thinning liquid, takes higher shear rate values as the bubble grows. Accordingly, the corresponding results obtained for viscosity distribution (Fig. 10) reveal that the viscosity of the stagnant liquid has decreases slightly (15-18mPa·s) as the bubble grows due to the shear thinning behavior.

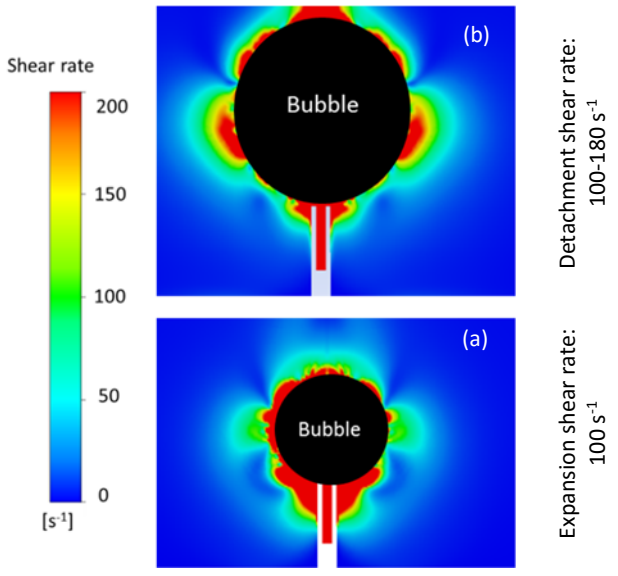

Figure 9: Shear rate distribution around a bubble during (a) expansion and (b) before detachment (*G2*), Q_G=0.10cm^3/s.

In particular, viscosity close to the bubble interface is lower than the corresponding value at zero-shear rate, according to the shear rate distribution. Numerical results show that viscosity values around the formated bubble do not reach the lower limit viscosity n_∞ (e.g at infinite shear rate), since the maximum shear rate is lower than 180s^{-1}. Also, the shear rate distribution decreases significantly as we approach the edges of the domain, i.e. where the liquid is not affected by the bubble growth, and the shear rate is practically zero.

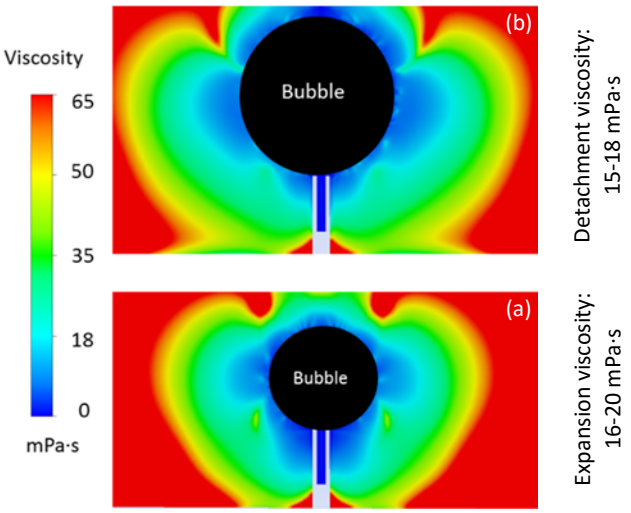

Figure 10: Viscosity distribution around a bubble during (a) expansion and (b) before detachment (*G2*), Q_G=0.10cm^3/s.

4. Concluding remarks

In this work we numerically investigated the shear rate distribution around a bubble that is formed in a non-Newtonian shear thinning liquid. Our aim was to explain the observation from our previous experimental work, i.e. that the behavior of a bubble column loaded with a shear thinning non-Newtonian liquid corresponds to that of a high viscosity Newtonian liquid. In turn, this means that the shear rates generated by the expanding and ascending bubbles must be relatively low.

The *CFD* simulations reveal that the shear rate around an under-formation bubble attains relatively low values (<180s^{-1}), that correspond to viscosities almost 100% greater than the relevant asymptotic viscosity value.

Furthermore, our experiments [3], which studied the coalescence of bubbles generated in non-Newtonian liquids from two neighboring μ-tubes, show that the coalescence frequency approaches practically zero even for the shortest distance (between the μ-tubes) tested. More *CFD* simulations concerning simultaneous bubble formation from two neighboring μ-tubes are currently in progress. Our intention is to estimate the shear rate distribution in the area between the two bubbles, in an effort to investigate the combined effect of the two bubbles on the flow field.

Acknowledgements: The authors would like to thank Dr. A.G. Kanaris for his fruitful comments and contribution to this work.

5. References

[1] Kazakis, N.A., Mouza, A.A., Paras, S.V., Coalescence during bubble formation at two neighboring pores: An experimental study in microscopic scale. *Chem. Eng. Sci.* **63,** 5160 – 5178, 2008.

[2] Loimer, T., Machu, G., Schaflinger, U., Inviscid bubble formation on porous plates and sieve plates. *Chem. Eng. Sci.* **59**, 809-818, 2004.

[3] Megari, A.I, Passos, A.D., Paras, S.V., Mouza, A.A., Experimental study of bubble formation and coalescence from neighboring micro-tubes in a non-Newtonian liquid. *10th Panhellenic Scientific Congress of Chemical Engineeering*, Patra, 2015 (*in greek*).

[4] Anastasiou, A.D., Passos, A., Mouza, A.A., Bubble columns with fine pore sparger and non-Newtonian liquid phase: Prediction of gas holdup. *Chem. Eng. Sci.* **98**, 331 – 338, 2013.

[5] Ohta, M., Iwasaki, E., Obata, E., Yoshida, Y., Dynamics processes in a deformed drop rising through shear-thinning fluids, *J. Non-Newton. Fluid*. **132**, 100–107, 2005.

[6] Islam, Md., Ganesan, P., Cheng, J., A pair of bubbles' rising dynamics in a xanthan gum solution: a CFD study, *R.S.C Adv*., **11**, 7803-7819, 2015.

[7] Zhang, L., Yang, C., Mao, Z., Numerical simulation of a bubble rising in shear-thinning fluids, *J. Non-Newton. Fluid*, **165**, 555-567, 2010.

[8] Chhabra, R.P., *Bubbles, Drops and Particles in non-Newtonian Fluids.* (2nd Ed.). Hoboken: Taylor & Francis Ltd. Pp. 18-20, 2006.

[9] Pourtousi, M., Ganesan, P., Kazemzadeh, A., Sandaran, S., Sahu, J.N., Methane bubble formation and dynamics in a rectangular bubble column: A CFD study, *Chemometr. Intell. Lab*., **147**, 2015.

[10] Hagesaether, L., Coalescence and break-up of drops and bubbles. Ph.D., Thesis, 2002.